Smart Structures and Systems, *Vol. 30, No. 2 (2022) 173-181*
https://doi.org/10.12989/sss.2022.30.2.173

Crack detection method for step-changed non-uniform beams using natural frequencies

Jong-Won Lee*

Department of Architectural Engineering, Namseoul University,
91 Daehak-ro, Seobuk-gu, Cheonan-si, Chungcheongnam-do 31020, Republic of Korea

(*Received August 9, 2021, Revised April 18, 2022, Accepted May 8, 2022*)

Abstract. The current paper presents a technique to detect crack in non-uniform cantilever-type pipe beams, that have step changes in the properties of their cross sections, restrained by a translational and rotational spring with a tip mass at the free end. An equation for estimating the natural frequencies for the non-uniform beams is derived using the boundary and continuity conditions, and an equivalent bending stiffness for cracked beam is applied to calculate the natural frequencies of the cracked beam. An experimental study for a step-changed non-uniform cantilever-type pipe beam restrained by bolts with a tip mass is carried out to verify the proposed method. The translational and rotational spring constants are updated using the neural network technique to the results of the experiment for intact case in order to establish a baseline model for the subsequent crack detection. Then, several numerical simulations for the specimen are carried out using the derived equation for estimating the natural frequencies of the cracked beam to construct a set of training patterns of a neural network. The crack locations and sizes are identified using the trained neural network for the 5 damage cases. It is found that the crack locations and sizes are reasonably well estimated from a practical point of view. And it is considered that the usefulness of the proposed method for structural health monitoring of the step-changed non-uniform cantilever-type pipe beam-like structures elastically restrained in the ground and have a tip mass at the free end could be verified.

Keywords: baseline model; crack detection; natural frequency; non-uniform; step-changed

1. Introduction

The cantilever-type pipe structures have been widely used in infrastructures, and those are usually elastically restrained in the ground and have a tip mass at the free end. Among those, there are non-uniform beams that have step changes in the properties of their cross sections in the longitudinal direction such as monopile support structures of offshore wind turbine. In the monopile support structure, the cross sectional properties are changed stepwise at the junction of the monopile substructure and the tower. And, the monopile support structure is restrained by the seabed ground and has a tip mass of blades and nacelle at the top of the tower.

Preventive maintenance and structural safety of those may be guaranteed by application of structural health monitoring system which can identify faults of the structures. The crack is one of the most typical damages in the steel pipe structures. It can be identified using the changes in modal properties of the structure resulting from the crack on the basis of the vibration data measured during operation. In the vibration-based crack detection method, if the model-based technique is applied to identify the crack, it is necessary to first update the baseline model that can analytically calculate the modal characteristics of the structures in intact state.

Several researches have been performed on the vibration of the non-uniform beams under various conditions. An exact solution to obtain the natural frequency and mode shape of non-uniform cantilever-type beams with multiple spring-mass systems was proposed (Chen and Wu 2002), the equation of motion was established by considering the compatibility of deformations and the equilibrium of forces between the two adjacent beam segments. A study on the vibration of the beams that have cross section geometries with exponentially varying width was performed (Ece *et al*. 2007), the governing equation was reduced to an ordinary differential equation and the modal characteristics for each set of boundary conditions were determined using the Euler–Bernoulli beam theory. A study was carried out to estimate the natural frequencies of the elastically restrained tapered beams with a tip mass and concentrated viscous damping at an arbitrary location (Rosa *et al*. 2010), the elastically restrained end was modeled as a translational and rotational spring element. An approach based on the Chebyshev polynomials theory was proposed to analyze free vibration of axially functionally graded Euler–Bernoulli and Timoshenko beams with non-uniform cross sections (Zhao *et al*. 2017), all variable geometric and material properties, such as cross sectional area, area moment of inertia, mass density, Young's modulus, and shear modulus were treated as weight functions. The asymptotic perturbation approach to obtain a simple analytical expression for the free vibration analysis of non-

*Corresponding author, Ph.D., Professor,
E-mail: jwlee.kimm@gmail.com

ISSN: 1738-1584 (Print), 1738-1991 (Online)

uniform and non-homogenous beams with different boundary conditions was applied (Cao *et al*. 2019), a linear governing equation of the beams was obtained based on the Euler–Bernoulli beam theory and the perturbative theory was employed to derive an asymptotic solution of the natural frequency of the beams. The dynamic stiffness matrix for generic non-uniform beams was formulated and applied to the free vibration analysis of flexure hinges (Ling *et al*. 2018), the vibration solution of general non-uniform Timoshenko beam was derived by using a recursive integral then, the dynamic stiffness matrix of non-uniform Timoshenko beam was derived based on the variational principle. The asymptotic development method was applied to analyze the free vibration of non-uniform axially functionally graded beams, of which the governing equations are differential equations with variable coefficients (Cao and Gao 2019), the perturbation theory was introduced to obtain an approximate analytical formula of the natural frequencies of the non-uniform beams with different boundary conditions. A study on the free vibration analysis of 3D non-uniform Euler-Bernoulli and Timoshenko beams by using the rigid segment method was performed (Nikolic and Salinic 2020), the elastic beam was discretized by 3 rigid segments which are connected by elastic joints with 6 degrees of freedom. The Rayleigh–Ritz method was used to analyze the vertical vibration of a non-prismatic mathematical hull with longitudinal distribution of sectional properties (Datta and Thekinen 2016), significant computational advantages of the proposed method over finite element analysis could be verified. Forced vibration of general non-uniform material-varying micro-beam models under a moving harmonic load/mass was studied (Rajasekaran and Khaniki 2019), cross section variation through the length was formulated for both thickness and width variation and material variation was modeled by combining axial and thickness material grading models. Vibrational properties of non-uniform beams made of graded porous materials was studied (Heshmati and Daneshmand 2019), the Timoshenko beam theory was used to formulate of the problem including non-uniformity of the cross section and graded porosity of the beam material. A theoretical method was proposed to investigate the natural vibration of non-uniform beams with derivable vibration mode function (Ma *et al*. 2020), the transfer matrix between the left and right cross sections of the cracked non-uniform beam was derived based on the vibration mode function.

In the previous studies, the methods for estimating the vibration characteristics of the non-uniform beams, that have continuous functionally varying cross sectional properties, have been mainly studied. In this study, an equation for estimating the natural frequencies for non-uniform beams, that have step changes in the properties of their cross sections, restrained by a translational and rotational spring with a tip mass at the free end is derived. Based on the equation, a technique to detect the location and size of a through-the-thickness crack in pipe using the natural frequencies and neural network technique is proposed. To this end, an equivalent bending stiffness for cracked beam is applied to the equation to calculate the natural frequencies of the cracked beam. The crack is assumed to be always open. An experimental study is carried out. The translational and rotational spring constants are updated to the results of the experiment for intact case to establish a baseline model for the subsequent crack detection. Then, several numerical simulations for the specimen are carried out to construct a set of training patterns of a neural network. The crack locations and sizes are identified using the trained neural network. To sum up, a technique to detect crack in non-uniform cantilever-type pipe beams, that have step changes in the properties of their cross sections, restrained by a translational and rotational spring with a tip mass is presented in this study.

2. Modal parameters of step-changed non-uniform beam

The general solution of the beam segments of constant cross sectional properties as shown in Fig. 1 can be expressed by individual functions as Eq. (1) and (2) (Gorman 1975). In Fig. 1, $r(\xi)$ is the transverse displacement, L is the beam length, E is the Young's modulus, I is the area moment of inertia, A is the cross sectional area, ρ is the mass density, k_T is the translational spring, k_R is the rotational spring, and M is the tip mass. The beam cross sectional properties are shown to be constant over the dimensionless distance μ from the supported end, and $\gamma = 1 - \mu$ for the remainder of the beam.

$$r_1(\xi_1) = A_1 sin\beta_1\xi_1 + B_1 cos\beta_1\xi_1 + C_1 sinh\beta_1\xi_1 + D_1 cosh\beta_1\xi_1 \quad (1)$$

$$r_2(\xi_2) = A_2 sin\beta_2\xi_2 + B_2 cos\beta_2\xi_2 + C_2 sinh\beta_2\xi_2 + D_2 cosh\beta_2\xi_2 \quad (2)$$

where

$$\beta_1^4 = \left(\frac{\rho_1 A_1}{E_1 I_1}\right)\omega^2 L^4 \quad (3)$$

$$\beta_2^4 = \left(\frac{\rho_2 A_2}{E_2 I_2}\right)\omega^2 L^4 \quad (4)$$

where ω is the natural circular frequency, and Eq. (5)-(7) can be introduced as follows

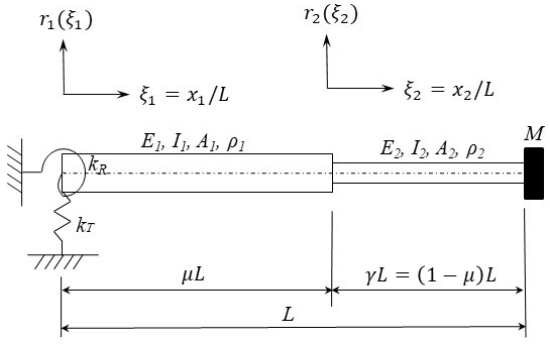

Fig. 1 Cantilever-type step-changed non-uniform beam with a tip mass and spring support

$$\varphi = \left(\frac{\rho_2 A_2}{\rho_1 A_1}\right)^{1/4} \tag{5}$$

$$\alpha = \left(\frac{E_2 I_2}{E_1 I_1}\right)^{1/4} \tag{6}$$

$$\lambda = \frac{\varphi}{\alpha} = \frac{\beta_2}{\beta_1} \tag{7}$$

The boundary conditions at the restrained end ($\xi_1 = 0$) and the free end ($\xi_2 = \gamma$) are as follows. Since the rotation angle at the free end of the cantilever-type beam used in large structures such as monopile support structure is often very small, the effect of rotational inertia caused by the tip mass is neglected in this study.

$$\left.\frac{d^2 r_1(\xi_1)}{d\xi_1^2}\right|_{\xi_1=0} = \frac{k_R L}{E_1 I_1}\left.\frac{dr_1(\xi_1)}{d\xi_1}\right|_{\xi_1=0} \tag{8}$$

$$\left.\frac{d^3 r_1(\xi_1)}{d\xi_1^3}\right|_{\xi_1=0} = -\frac{k_T L^3}{E_1 I_1}\left.r_1(\xi_1)\right|_{\xi_1=0} \tag{9}$$

$$\left.\frac{d^2 r_2(\xi_2)}{d\xi_2^2}\right|_{\xi_2=\gamma} = 0 \tag{10}$$

$$\left.\frac{d^3 r_2(\xi_2)}{d\xi_2^3}\right|_{\xi_2=\gamma} = -\frac{M}{\rho_2 A_2 L}\beta_2^4 \left.r_2(\xi_2)\right|_{\xi_2=\gamma} \tag{11}$$

The continuity conditions of displacement, slope, bending moment, and shear force at the variation location of the cross sectional properties ($\xi_1 = \mu$, $\xi_2 = 0$) are as follows

$$r_1(\mu) = r_2(0) \tag{12}$$

$$\left.\frac{dr_1(\xi_1)}{d\xi_1}\right|_{\xi_1=\mu} = \left.\frac{dr_2(\xi_2)}{d\xi_2}\right|_{\xi_2=0} \tag{13}$$

$$\left.\frac{d^2 r_1(\xi_1)}{d\xi_1^2}\right|_{\xi_1=\mu} = \alpha^4 \left.\frac{d^2 r_2(\xi_2)}{d\xi_2^2}\right|_{\xi_2=0} \tag{14}$$

$$\left.\frac{d^3 r_1(\xi_1)}{d\xi_1^3}\right|_{\xi_1=\mu} = \alpha^4 \left.\frac{d^3 r_2(\xi_2)}{d\xi_2^3}\right|_{\xi_2=0} \tag{15}$$

A coefficient matrix equation for the unknown $A_1, B_1, C_1, D_1, A_2, B_2, C_2, D_2$ in Eqs. (1) and (2) can be obtained by applying the above boundary and continuity conditions. For a non-trivial solution, the determinant of the coefficient matrix is set to zero as follows

$$\begin{vmatrix} E_{11} & E_{12} & E_{13} & E_{14} & 0 & 0 & 0 & 0 \\ E_{21} & E_{22} & E_{23} & E_{24} & 0 & 0 & 0 & 0 \\ 0 & 0 & 0 & 0 & E_{35} & E_{36} & E_{37} & E_{38} \\ 0 & 0 & 0 & 0 & E_{45} & E_{46} & E_{47} & E_{48} \\ E_{51} & E_{52} & E_{53} & E_{54} & 0 & -1 & 0 & -1 \\ E_{61} & E_{62} & E_{63} & E_{64} & E_{65} & 0 & E_{67} & 0 \\ E_{71} & E_{72} & E_{73} & E_{74} & 0 & E_{76} & 0 & E_{78} \\ E_{81} & E_{82} & E_{83} & E_{84} & E_{85} & 0 & E_{87} & 0 \end{vmatrix} = 0 \tag{16}$$

where

$$E_{11} = E_{13} = \frac{k_R L}{E_1 I_1} \tag{17}$$

$$E_{12} = -E_{14} = \beta_1 \tag{18}$$

$$E_{21} = -E_{23} = \beta_1^3 \tag{19}$$

$$E_{24} = E_{22} = -\frac{k_T L^3}{E_1 I_1} \tag{20}$$

$$E_{35} = sin\lambda\beta_1\gamma \tag{21}$$

$$E_{36} = cos\lambda\beta_1\gamma \tag{22}$$

$$E_{37} = -sinh\lambda\beta_1\gamma \tag{23}$$

$$E_{38} = -cosh\lambda\beta_1\gamma \tag{24}$$

$$E_{45} = cos\lambda\beta_1\gamma - \frac{M}{\rho_2 A_2 L}\lambda\beta_1 sin\lambda\beta_1\gamma \tag{25}$$

$$E_{46} = -sin\lambda\beta_1\gamma - \frac{M}{\rho_2 A_2 L}\lambda\beta_1 cos\lambda\beta_1\gamma \tag{26}$$

$$E_{47} = -cosh\lambda\beta_1\gamma - \frac{M}{\rho_2 A_2 L}\lambda\beta_1 sinh\lambda\beta_1\gamma \tag{27}$$

$$E_{48} = -sinh\lambda\beta_1\gamma - \frac{M}{\rho_2 A_2 L}\lambda\beta_1 cosh\lambda\beta_1\gamma \tag{28}$$

$$E_{51} = -E_{62} = E_{71} = -E_{82} = sin\beta_1\mu \tag{29}$$

$$E_{52} = E_{61} = E_{72} = E_{81} = cos\beta_1\mu \tag{30}$$

$$E_{53} = E_{64} = -E_{73} = -E_{84} = sinh\beta_1\mu \tag{31}$$

$$E_{54} = E_{63} = -E_{74} = -E_{83} = cosh\beta_1\mu \tag{32}$$

$$E_{65} = E_{67} = -\lambda \tag{33}$$

$$E_{76} = -E_{78} = -\alpha^4\lambda^2 \tag{34}$$

$$E_{85} = -E_{87} = -\alpha^4\lambda^3 \tag{35}$$

Then, β_1 satisfying Eq. (16) can be calculated, and the natural frequency can be obtained by substituting the β_1 into Eq. (3).

The mode shape of the beam can be defined by substituting the β_1 into the coefficient matrix equation from which Eq. (16) is set and using the reduced row echelon form of the coefficient matrix equation.

The natural frequencies and mode shapes for an example step-changed non-uniform beam of which the material is steel as shown in Fig. 2, the same dimension as the specimen for subsequent experimental study, are calculated.

The cross section of the 2 segments is the pipe, the outer diameter of the 2 segments is 139.8 mm, the thicknesses of

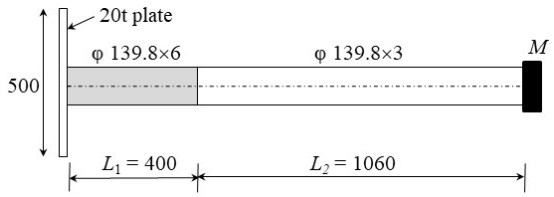

Fig. 2 Dimension of the example beam (lengths in mm)

the left and right segment are 6 mm and 3 mm, respectively, the total length is 1,460 mm, $\mu = 0.274$, $\gamma = 0.726$, $E = 2.1 \times 10^{11}$ Pa, $\rho = 7{,}850$ kg/m^3, and $M = 5.65$ kg. The 20t plate in Fig. 2 is assumed to be restrained by a translational and rotational spring, and k_T and k_R are set to 1.3473×10^7 N/m and 8.3183×10^5 N.m, respectively. These spring constants are the results of updating the baseline model for the specimen which is subsequently carried out.

The calculated natural frequencies using Eq. (3) agree well with those obtained from a general finite element analysis program as shown in Table 1. The calculated mode shapes normalized by the norms are shown in Fig. 3.

3. Natural frequency of cracked beam

The equivalent bending stiffness was constructed on the basis of the energy method for the cracked uniform pipe (Yang *et al*. 2001, Swamidas *et al*. 2004, Lee *et al*. 2014) as follows

$$EI_c = \frac{EI}{1 + \frac{EIR(\theta,c)}{\left\{1+\left(\frac{x-c}{k(\theta)\theta}\right)^2\right\}}} \quad \left(0 < \theta \le \frac{\pi}{2}\right) \tag{36}$$

where EI_c is the equivalent bending stiffness of the cracked beam, EI is the bending stiffness of the un-cracked beam, θ is the crack size as shown in Fig. 4, and c is the distance to the crack location from the restrained end in Fig. 1. Hence, the equivalent bending stiffness of the cracked beam can be defined by the distance along the beam x, the crack location c, and the crack size θ using Eq. (36).

Also, in Eq. (36) for understanding

$$R(\theta, c) = \frac{2D(\theta)}{k(\theta)\theta j(\theta, c)} \tag{37}$$

$$k(\theta) = \frac{2\sqrt{2}R(1-\nu^2)iG(\theta)}{\pi^2 \epsilon \theta}\left(\frac{I_c}{I - I_c}\right) \tag{38}$$

Table 1 Natural frequencies of the example beam (Hz)

Mode no.	Using Eq. (3)	Using FEM program
1	25.589	25.587
2	168.248	168.246
3	404.582	404.574
4	997.920	997.901

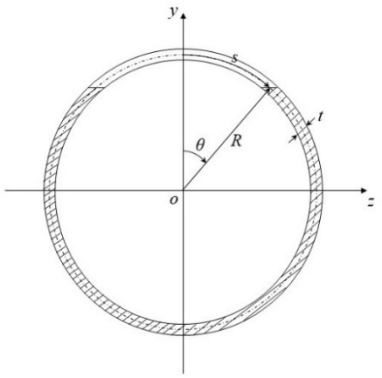

Fig. 4 Configuration of cracked section (Lee *et al*. 2014)

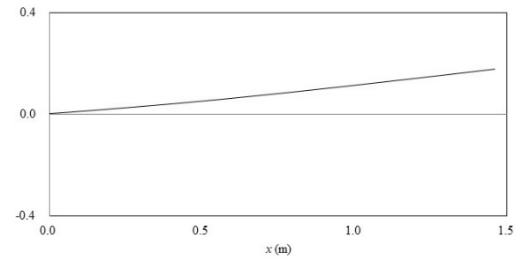

(a) 1st mode

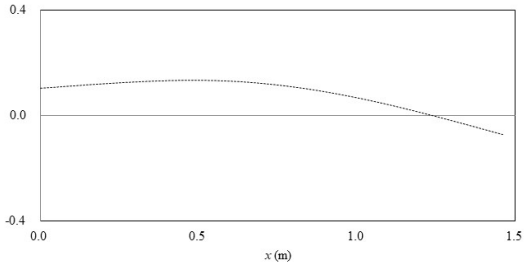

(b) 2nd mode

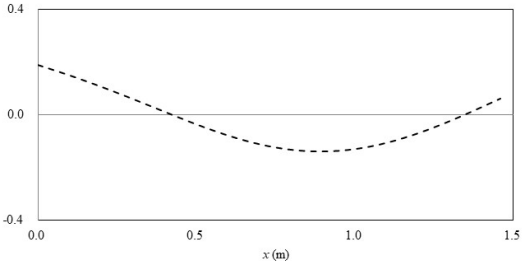

(c) 3rd mode

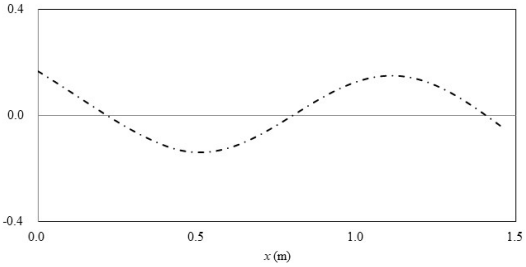

(d) 4th mode

Fig. 3 Mode shapes of the example beam

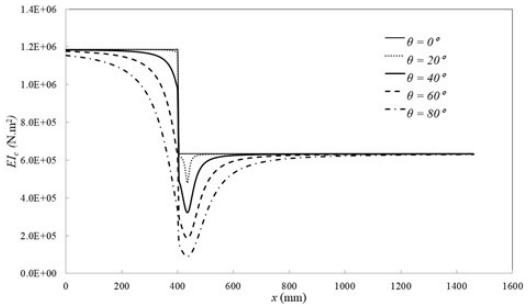

Fig. 5 Variation of the equivalent bending stiffness for the cracked beam

$$D(\theta) = \frac{\sqrt{2}(1-\nu^2)iG(\theta)}{\pi^2 ER^2 t\varepsilon} \tag{39}$$

$$j(\theta, c) = arctan\left(\frac{L-c}{k(\theta)\theta}\right) + arctan\left(\frac{c}{k(\theta)\theta}\right) \tag{40}$$

$$G(\theta) = sin\theta\left[1 + \frac{1}{2}\frac{\theta - cot(1-\theta cot\theta)}{2cot\theta + \sqrt{2}cot\left(\frac{\pi-\theta}{\sqrt{2}}\right)}\right] \tag{41}$$

$$iG(\theta) = \int_0^{\theta} G(\theta)^2 d\theta \tag{42}$$

$$\varepsilon^2 = \left(\frac{t}{R}\right)/\sqrt{12(1-\nu^2}} \tag{43}$$

where $R(\theta, c)$, $k(\theta)$, $D(\theta)$, and $j(\theta, c)$ are the arbitrary functions, $G(\theta)$ is the configuration function for crack opening area in circular hollow section, ν is the Poisson's ratio, R is the average of the inner and outer radii in the cracked section, t is the thickness of the pipe, and I_c is the area moment of inertia of the cracked section.

Fig. 5 shows the variation of the equivalent bending stiffness along the beam length calculated from Eq. (36) when the crack location (c/L) is 0.298 (the location of 435 mm from the 20t plate) for the beam shown in Fig. 2. The cracks are inflicted at this location in later experimental study. It can be found that the equivalent bending stiffness is changed stepwise at the variation location ($x = 0.4$ m) of the cross sectional properties when θ is zero. It can be found that the stiffness reduction is highly concentrated near the crack location, and reach zero at a location far away from the crack. It can be also found that the stiffness reduction near the crack location becomes lager as the crack size increases.

To solve the vibration equation for Euler beam, an integral type characteristic equation based on the Galerkin's method can be obtained as follows

$$\begin{aligned}
&\int_0^{\mu L}\left[\frac{d^2\phi_i(x_1)}{dx_1^2}E_1I_1(x_1)_c\frac{d^2\phi_j(x_1)}{dx_1^2}\right]dx_1 \\
&+\int_0^{\gamma L}\left[\frac{d^2\phi_i(x_2)}{dx_2^2}E_2I_2(x_2)_c\frac{d^2\phi_j(x_2)}{dx_2^2}\right]dx_2 \\
&+\frac{d\phi_i(x_1)}{dx_1}\bigg|_{x_1=0}k_R\frac{d\phi_j(x_1)}{dx_1}\bigg|_{x_1=0} \\
&+\phi_i(x_1)|_{x_1=0}k_T\phi_i(x_1)|_{x_1=0} \\
&-\omega_c^2\left\{\rho_1A_1\int_0^{\mu L}\phi_i(x_1)\phi_j(x_1)dx_1\right. \\
&+\rho_2A_2\int_0^{\gamma L}\phi_i(x_2)\phi_j(x_2)dx_2 \\
&\left.+\phi_i(x_2)|_{x_2=\gamma L}M\phi_j(x_2)\big|_{x_2=\gamma L}\right\} = 0
\end{aligned} \tag{44}$$

where ω_c is the natural circular frequency of the cracked beam and $\phi_i(x)$ is the i^{th} mode shape. Therefore, the natural frequencies of the cracked beam can be calculated by the numerical integration for Eq. (44).

Fig. 6 shows the normalized natural frequencies for various crack locations when the crack is occurred in the beam shown in Fig. 2 with the size (θ) of 60°. The crack occurring near the free end of the beam affects little on the

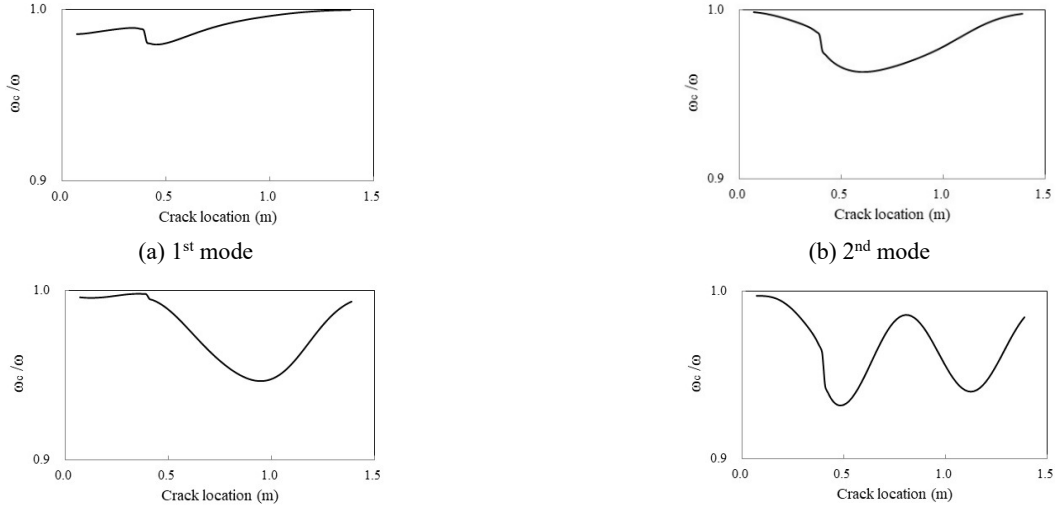

(a) 1st mode (b) 2nd mode

(c) 3rd mode (d) 4th mode

Fig. 6 Variation of the natural frequencies as a function of crack location

frequency change. It can be found that the decrement of the frequency due to the crack is sharply changed at the variation location ($x = 0.4$ m) of the cross sectional properties. It can be also found that the variation of the frequency as a function of crack location for each mode is different depending on the mode shape.

4. Updating the baseline model

In order to estimate damage by using the vibration and model-based technique, it is necessary to update the baseline model that can analytically obtain the modal characteristics of the structure in healthy state.

A step-changed non-uniform cantilever-type pipe beam was built to verify the present technique as shown in Fig. 7. The dimensions and material of this specimen are the same as those in Fig. 2, and a tip mass of 5.65 kg was added at the free end. The 20 t plate in Fig. 2 was fastened using high tensile bolts to a foundation block as shown in Fig, 7, and this block was bonded to the laboratory floor.

In the specimen, 2 steel pipes with the same outer diameter but different thicknesses were joined by groove welding. In this study, a natural frequency estimation and crack detection technique has been researched assuming an ideal groove welding joint. However, structural characteristics of joint such as rigidity and strength can be changed depending on the connection method and condition, so it is difficult to accurately model it. It is thought that this issue should be considered in additional studies for the practical use of the technique in the future.

Fig. 7 Experimental setup

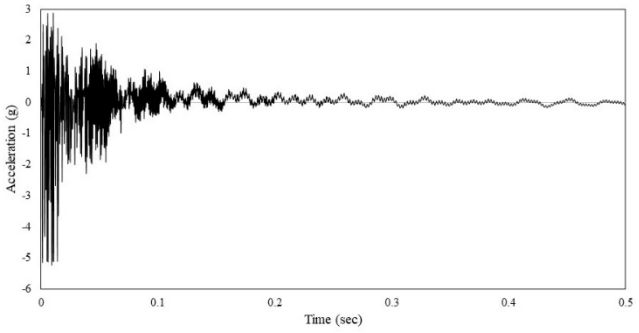

Fig. 8 Acceleration time history

The free vibration tests were performed 10 times for the intact case using the impact hammer method. For mode discrimination, 4 accelerometers were installed at the restrained end, 0.73 m and 1.095 m from the restrained end, and at the free end. The accelerations were measured with the sampling rate of 5,000 Hz, and the first 3 natural frequencies were obtained using the frequency domain decomposition method and averaging the results of the 10 free vibration tests. A time history of the acceleration measured by the accelerometer installed at the free end is shown in Fig. 8.

The experimental results are compared with those calculated with the fixed end boundary condition in Table 2. The reason for the difference between the two could be attributed to the assumption that fastening with the high tensile bolts cannot become a complete fixed end but an elastically restrained end. Therefore, it can be assumed that the beam was restrained with the translational spring k_T and rotational spring k_R as shown in Fig. 1. That is, the translational and rotational spring effects at the restrained end were determined to have large uncertainties compared to the rigidity of the structural member itself, so it was set as a variable to update the baseline model. In the case of cantilever-type beams such as monopile support structure of offshore wind turbine, the restrained end is elastically supported by the soil, and it is considered that this restraint effect of the soil is uncertain compared to the rigidity of the structure itself. The spring constants were initially set-up as $k_T^i = 0.075 \times \frac{12E_1I_1}{L_1^3}$ N/m and $k_R^i = 0.075 \times \frac{4E_1I_1}{L_1}$ N.m, respectively using a trial and error method. The natural frequencies applying these initial spring constants were calculated using Eq. (3) and are compared in Table 2. These results are still different to the experimental results.

The initial translational and rotational spring constant were updated to the experimental results using the neural network technique. The neural network technique used

Table 2 Natural frequencies of the specimen (unit: Hz)

Mode no.	1	2	3
Experiment	25.635	168.460	406.494
Calculated w/o springs (fixed end)	49.415 (92.76)	352.643 (109.33)	980.866 (141.30)
Calculated w/ springs (initial) $k_T^i = 0.075 \times \frac{12E_1I_1}{L_1^3}$ $k_R^i = 0.075 \times \frac{4E_1I_1}{L_1}$	26.294 (2.57) [2.77]	178.249 (5.81) [5.31]	421.721 (3.75) [2.65]
Calculated w/ springs (updated) $k_T = 0.807 \times k_T^i$ $k_R = 0.934 \times k_R^i$	25.589 (0.18) [0.19]	168.248 (0.13) [0.12]	404.582 (0.47) [0.33]

Note 1: The values in brackets are errors for the experimental results in %.
Note 2: The values in square brackets are error ratios for the calculated results w/o springs (fixed end)

here is described in Chapter 5. That is, 300 sets of the translational and rotational spring constant were randomly sampled, and the first 3 natural frequencies were calculated for the 300 sets, then the 300 training patterns were generated. Each training pattern consists of the translational and rotational spring constant and their corresponding natural frequencies for the first 3 modes. The first 3 natural frequencies were used as the input data to a neural network, 2 hidden layers with 4 and 3 nodes each were introduced, and the output layer was composed of the translational and rotational spring constant. Training was carried out by using the established training patterns, and the translational and rotational spring constant were estimated as $k_T = 0.807 \times k_T^i$ and $k_R = 0.934 \times k_R^i$. The natural frequencies applying these updated spring constants were calculated using Eq. (3) and are compared in Table 2. It can be found that these results are in good agreement with the experimental results. These updated results are used in the subsequent crack detection.

5. Crack identification

Estimation of the crack location and size was experimentally carried out for the specimen in Fig. 7 to verify the present method. The cracks were inflicted by making fine saw cuts of the beam shown in Fig. 9 at the location of 435 mm (c/L = 0.298) from the restrained end. Five cases of damages (θ = 10.96°, 23.72°, 35.82°, 48.26°, and 59.68°) were introduced by changing the depth of the inflicted crack.

The free vibration tests were performed 10 times for each of the 5 damage cases using the impact hammer method. Test methods such as the number and location of accelerometers and sampling rate are same as those for the intact case, and the first 3 natural frequencies were obtained for each damage case.

A multilayer perceptron neural network, which is one of the feedforward neural network, is used for identification of the crack location and size. The input/output relationship of the neural network can be nonlinear as well as linear, and its characteristics are determined by the synaptic weights assigned to the connections between the neurons in two adjacent layers. Systematic way of updating the weights to achieve a desired input/output relationship based on a set of training patterns is referred as training or learning algorithm. In this study, the standard back-propagation algorithm is used.

A set of training patterns for a neural network was generated by sampling several damage cases for the crack location and size, and calculating the corresponding natural frequencies using Eq. (44) with the updated translational and rotational spring in Chapter 4. Then, the neural network was trained using the training patterns, and the crack could be identified by inputting the measured natural frequencies to the trained neural network. That is, 2000 sets of the crack location and size were randomly sampled, and the first 3 natural frequencies were numerically computed for the 2000 sets of the damage cases. Then, the 2000 training patterns were generated, and each training pattern consisted of the crack location and size and their corresponding ratios of the natural frequencies between before and after the damage for the first 3 modes.

The frequency ratios for the first 3 modes were used as the input data to the neural network, which resulted in 3 nodes in the input layer. Two hidden layers with 3 nodes each were introduced. The output layer was composed of the crack location and size which resulted in 2 nodes. The structure of the neural network is shown in Fig. 10.

Training of the neural network was carried out by using the training patterns for 100 epochs to obtain a stable estimation error and incorporating the noise injection learning algorithm to reduce the effects of measurement noise. In the noise injection learning algorithm, the training is carried out using the artificially contaminated training patterns with noise of a prescribed level. The generalization capability of the neural network can be enforced through this algorithm, because this algorithm has similar effect to the regularization technique that is used to mollify the ill-

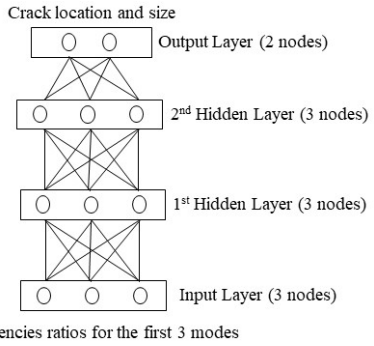

Fig. 10 Structure of the neural network

Fig. 9 Inflicted crack (θ = 23.72°)

Table 3 Estimated crack locations and sizes

Case	Crack size, θ (degree)		Crack location, c/L	
	Accurate	Estimated	Accurate	Estimated
1	10.96	21.96 (100.29)	0.298	0.384 (28.86)
2	23.72	32.94 (38.84)	0.298	0.295 (1.01)
3	35.82	49.50 (38.20)	0.298	0.285 (4.36)
4	48.26	52.56 (8.91)	0.298	0.290 (2.68)
5	59.68	68.76 (15.22)	0.298	0.293 (1.68)

Note: The values in brackets are errors for the accurate ones in %

posedness of the inverse problems (Matsuoka 1992). The level of the noise considered in the noise injection learning was 3% for the first 3 frequencies, respectively. Table 3 shows the estimated crack locations and sizes for the 5 damage cases using the neural network.

The crack sizes are slightly overestimated for the all damage cases. In the future, the estimation error for the crack size could be reduced if the accuracy of the equivalent bending stiffness distribution of cracked beams in Eq. (36) is improved through experimental studies on the relevant cross section and material. The trouble during structural health monitoring is supposed to be underestimating the actual damage severity or failing to detect the occurrence of damage. Compared to these cases, it is regarded that the problem of overestimation can be relatively less important from a practical point of view. Besides, if repair and reinforcement are performed conservatively based on the overestimated crack size, the safety of the structure may not be affected.

It can be found that all of the crack locations are detected reasonably except for Case 1 which is a case of relatively small damage. In the case of a small damage, the natural frequency change due to damage is small, and this change can be affected relatively much by noise. That is, the smaller the crack size, the larger the error of the estimation identified using the change in natural frequency due to crack. Since it is important to detect small damage, it is considered that this problem should be solved by applying smart sensors and solving noise problems in the future. However, it can be found that for all other damage cases, the crack locations are successfully estimated. For practical application, the accuracy of the estimated damage severities may be less important, as long as the damage locations can be detected successfully. That is, if the crack location can be reasonably estimated during structural health monitoring, effective repair and reinforcement are possible through detailed inspection of the location. Over all, this result indicates the usefulness of the proposed method for structural health monitoring of the non-uniform cantilever-type pipe beams, that have step changes in the properties of their cross sections, restrained by a translational and rotational spring with a tip mass at the free end.

In this study a baseline model has been updated in Chapter 4 to the experimental results in healthy state that can analytically obtain the natural frequencies of the specimen, and used in the generation of the training patterns of the neural network. Therefore, it can be supposed that if the test results for intact case are input, no crack result will be output. Actually, a very small crack size of 0.54° was estimated as a result of inputting the natural frequencies for intact case into the same neural network used in the crack detection.

It is known that the mode shape is more sensitive to the local damage than the natural frequency, and if the mode shape information is used together, the accuracy of the damage estimation can be improved. However, in this study an integral type characteristic equation (Eq. (44)) which can estimate the natural frequencies of non-uniform cracked beams, that have step changes in the properties of their cross sections, restrained by a translational and rotational spring with a tip mass at the free end has been induced. A set of training patterns for a neural network was generated by sampling several damage cases for the crack location and size, and calculating the corresponding natural frequencies using Eq. (44). Then, the neural network was trained using the training patterns, and used to detect crack location and size. In order to use the mode shape information, it is necessary to study additionally on a method to obtain the mode shape for cracked beams under the same conditions described above.

The strengths of the proposed analytical model compared to the finite element method are supposed to be as follows. If the proposed analytical model is used, various damage models can be applied to the analytical model, and the structural response for multiple damage cases can be calculated using this. For the accuracy of damage estimation based on the neural network technique, it is necessary to calculate the structural response for considerably multiple damage cases, and it is supposed to be more advantageous than the finite element method in terms of the computing time.

6. Conclusions

This study presents a method that can estimate the natural frequency of non-uniform beams, that have step changes in the properties of their cross sections, restrained by a translational and rotational spring with a tip mass at the free end, and detect crack in the step-changed non-uniform cantilever-type pipe beams. Most of the existing methods to estimating the vibration characteristics of the non-uniform beams reported in the literature have been researched for the beams that have continuous functionally varying cross sectional properties.

An equation for estimating the natural frequencies was derived using the boundary and continuity conditions, and an equivalent bending stiffness for cracked beam was applied to the equation to calculate the natural frequencies of the cracked beam. An experimental study was carried out to verify the proposed method. Updating a baseline model for a step-changed non-uniform cantilever-type pipe beam restrained elastically with a tip mass at the free end was carried out before detecting the crack. This technique could be useful for updating the baseline model for model-based damage estimation of the real structure elastically restrained in the ground and has a tip mass such as monopile support structure of offshore wind turbine. Crack identifications were carried out for the 5 damage cases experimentally using the neural network technique. The crack sizes were slightly overestimated for the all damage cases. This estimation error for the crack size could be reduced if the accuracy of the equivalent bending stiffness distribution of cracked beams is improved through experimental studies in the future. However, compared to the cases of underestimating or failing to detect the actual damage, it is regarded that the problem of overestimation can be relatively less important from a practical point of view. The crack locations were detected reasonably except for a case of relatively small damage. Since it is important to detect small damage, it is considered that this problem should be

solved by applying smart sensors and solving noise problems in the future. However, the crack locations were successfully estimated for all other damage cases. These results of the crack identification support the usefulness of the proposed method in this study for structural health monitoring of the step-changed non-uniform cantilever-type pipe beam-like structures.

Further researches might address such issues as improvement of accuracy for small crack estimation and reduction of crack size identification error. Also, it is expected that the proposed technique could be extended to the non-uniform beams composed of a uniform and a tapered cross section like the monopile support structure of offshore wind turbine. In addition, it is supposed that further research is needed on the technique using the mode shape together and the more accurate modeling method for the joint.

Acknowledgments

This research was supported by Korea Electric Power Corporation. (Grant number: R20XO02-30)

References

Cao, D. and Gao, Y. (2019), "Free vibration of non-uniform axially functionally graded beams using the asymptotic development method", *Appl. Mathe. Mech.*, **40**, 85-96. http://dx.doi.org/10.1007/s10483-019-2402-9

Cao, D., Gao, Y., Wang, J., Yao, M. and Zhang, W. (2019), "Analytical analysis of free vibration of non-uniform and non-homogenous beams: Asymptotic perturbation approach", *Appl. Mathe. Modell.*, **65**, 526-534. http://dx.doi.org/10.1016/j.apm.2018.08.026

Chen, D.W. and Wu, J.S. (2002), "The exact solutions for the natural frequencies and mode shapes of non-uniform beams with multiple spring-mass systems", *J. Sound Vib.*, **255**, 299-322. http://dx.doi.org/10.1006/jsvi.2001.4156

Datta, N and Thekinen, J.D. (2016), "A Rayleigh–Ritz based approach to characterize the vertical vibration of non-uniform hull girder", *Ocean Eng.*, **125**, 113-123. http://dx.doi.org/10.1016/j.oceaneng.2016.07.046

Ece, M.C., Aydogdu, M. and Taskin, V. (2007), "Vibration of a variable cross-section beam", *Mech. Res. Commun.*, **34**, 78-84. http://dx.doi.org/10.1016/j.mechrescom.2006.06.005

Gorman, D.J. (1975), *Free Vibration Analysis of Beams and Shafts*, John Wiley & Sons, New York, NY, USA.

Heshmati, M. and Daneshmand, F. (2019), "Vibration analysis of non-uniform porous beams with functionally graded porosity distribution", *Proceedings of the Institution of Mechanical Engineers, Part L: Journal of Materials: Design and Applications*, **233**, 1678-1697. https://doi.org/10.1177/1464420718780902

Lee, J.W., Kim, S.R. and Huh, Y.C. (2014), "Pipe crack identification based on the energy method and committee of neural networks", *Int. J. Steel Struct.*, **14**, 345-354. http://dx.doi.org/10.1007/s13296-014-2014-0

Ling, M., Chen, S., Li, Q. and Tian, G. (2018), "Dynamic stiffness matrix for free vibration analysis of flexure hinges based on non-uniform Timoshenko beam", *J. Sound Vib.*, **437**, 40-52. http://dx.doi.org/10.1016/j.jsv.2018.09.013

Ma, Y., Du, X., Chen, G. and Yang, F. (2020), "Natural vibration of a non-uniform beam with multiple transverse cracks", *J. Brazil. Soc. Mech. Sci. Eng.*, **42**, 161. https://doi.org/10.1007/s40430-020-2246-1

Matsuoka, K. (1992), "Noise injection into inputs in back-propagation", *IEEE Transact. Syst. Man Cybernet.*, **22**, 436-440. http://dx.doi.org/10.1109/21.155944

Nikolic, A. and Salinic, S. (2020), "Free vibration analysis of 3D non-uniform beam: the rigid segment approach", *Eng. Struct.*, **222**, 110796. https://doi.org/10.1016/j.engstruct.2020.110796

Rajasekaran, S. and Khaniki, H.B. (2019), "Size-dependent forced vibration of non-uniform bi-directional functionally graded beams embedded in variable elastic environment carrying a moving harmonic mass", *Appl. Mathe. Modell.*, **72**, 129-154. https://doi.org/10.1016/j.apm.2019.03.021

Rosa, M.A.D., Lippiello, M., Maurizi, M.J. and Martin, H.D. (2010), "Free vibration of elastically restrained cantilever tapered beams with concentrated viscous damping and mass", *Mech. Res. Commun.*, **37**, 261-264. https://doi.org/10.1016/j.mechrescom.2009.11.006

Swamidas, A.S.J., Yang, X.F. and Seshadri, R. (2004), "Identification of cracking in beam structures using Timoshenko and Euler formulations?, *J. Eng. Mech.*, **130**, 1297-1308. http://dx.doi.org/10.1061/(ASCE)0733-9399(2004)130:11(1297)

Yang, X.F., Swamidas, A.S.J. and Seshadri, R. (2001), "Crack identification in vibrating beams using the energy method", *J. Sound Vib.*, **244**, 339-357. http://dx.doi.org/10.1006/jsvi.2000.3498

Zhao, Y., Huang, Y. and Guo, M. (2017), "A novel approach for free vibration of axially functionally graded beams with non-uniform cross-section based on Chebyshev polynomials theory", *Compos. Struct.*, **168**, 277-284. http://dx.doi.org/10.1016/j.compstruct.2017.02.012

HJ